Laminar and columnar auditory cortex in avian brain

Yuan Wang[a,b,1], Agnieszka Brzozowska-Prechtl[a], and Harvey J. Karten[a]

[a]Department of Neurosciences, School of Medicine, University of California San Diego, La Jolla, CA 92093-0608; and [b]Department of Otolaryngology and Virginia Merrill Bloedel Hearing Research Center, University of Washington, Seattle, WA 98195-7923

Communicated by Melvin I. Simon, California Institute of Technology, Pasadena, CA, June 2, 2010 (received for review January 27, 2010)

The mammalian neocortex mediates complex cognitive behaviors, such as sensory perception, decision making, and language. The evolutionary history of the cortex, and the cells and circuitry underlying similar capabilities in nonmammals, are poorly understood, however. Two distinct features of the mammalian neocortex are lamination and radially arrayed columns that form functional modules, characterized by defined neuronal types and unique intrinsic connections. The seeming inability to identify these characteristic features in nonmammalian forebrains with earlier methods has often led to the assumption of uniqueness of neocortical cells and circuits in mammals. Using contemporary methods, we demonstrate the existence of comparable columnar functional modules in laminated auditory telencephalon of an avian species (*Gallus gallus*). A highly sensitive tracer was placed into individual layers of the telencephalon within the cortical region that is similar to mammalian auditory cortex. Distribution of anterograde and retrograde transportable markers revealed extensive interconnections across layers and between neurons within narrow radial columns perpendicular to the laminae. This columnar organization was further confirmed by visualization of radially oriented axonal collaterals of individual intracellularly filled neurons. Common cell types in birds and mammals that provide the cellular substrate of columnar functional modules were identified. These findings indicate that laminar and columnar properties of the neocortex are not unique to mammals and may have evolved from cells and circuits found in more ancient vertebrates. Specific functional pathways in the brain can be analyzed in regard to their common phylogenetic origins, which introduces a previously underutilized level of analysis to components involved in higher cognitive functions.

neocortex evolution | columnar organization | primary auditory cortex | intrinsic circuitry | granule cell

The origins and evolution of the forebrain and the mammalian neocortex,* where complex cognitive functions are centered, have long been of broad interest to scientists and nonscientists alike. For more than 100 y, the neocortex was considered an independently evolved structure unique to mammals. The nonmammalian telencephalon was frequently compared with the mammalian basal ganglia, which was thought to be involved in stereotypical instinctive behaviors (1). A revolutionary revision in our concept of the nature of vertebrate brain organization was recently accepted in the revised nomenclature of the avian brain (2, 3). The avian Wulst and dorsal ventricular ridge, two prominent components of the telencephalon, are recognized as being homologous to pallial components of mammalian brains, which is consistent with the idea that avian telencephalon includes a large cortical component (Fig. 1 *A*–*C*) (4–6). However, this postulated homology addresses only the most general aspects of the evolutionary relationship of the avian brain to the mammal brain, that is, in indicating that birds have some form of generic cortex. Whether or not discrete cell groups in the avian pallial telencephalon are homologous to the neocortex or noncortical (claustrum and amygdala) mammalian pallium remains controversial.

The proposal that the avian dorsal ventricular ridge contains populations of neurons and circuits homologous to those of the mammalian neocortex was initially suggested in the 1960s on the basis of similarities in neurotransmitter distribution and patterns of afferent connectivity (7–10). Major sensory ascending projections through the thalamus and then on the telencephalon of birds and reptiles demonstrated the antiquity of these pathways in amniotes and led to the hypothesis that distinct nuclei of the avian and reptilian telencephalon were homologous to morphologically and physiologically corresponding laminae of the mammalian neocortex. This nucleus to lamina homology is further supported by remarkable similarities in cell morphology, intratelencephalic connections, gene expression, and functions between specific nuclei in birds and corresponding laminae in mammals (4–6, 11–16).

A more critical question, however, is whether these nuclei and their neurons are interconnected in a similar pattern to form circuitry with similar intrinsic operational mechanism as those of the mammalian neocortex. Two of the most distinct features of the mammalian neocortex are its laminar architecture and columnar organization, features that underlie the essential computational mechanisms vital to their postulated functions (17–24). The mammalian neocortex is characterized by the presence of defined cell types arranged in six parallel laminae with distinctive neuronal connections organized in radial columns. Among these, layer IV receives a topographically organized input from the thalamus and redistributes the information to other layers through radially arrayed intrinsic connections between layers. Consequently, neurons included in a cylinder oriented perpendicularly to layers tend to have some specific functional properties in common and are believed to constitute local computational units (19, 22), although how this columnar organization contributes to cortical function is not completely understood (25, 26).

In contrast, the cortical region of birds, as well as that of reptiles, lacks the obvious laminar appearance of uniformly parallel layers and has long been considered to be organized in a cluster pattern, that is, individual nuclei of the avian telencephalon having unitary functions. A lack of pertinent information that might address this question significantly weakens the argument that the avian cortex is organized in a manner similar to the mammalian neocortex, and has been used to justify an alternative view postulating homology to noncortical structures of the mammalian pallium (27–31). These proposals argue that the reported similarities between the nonmammalian pallium and the mammalian neocortex could be independently evolved in the absence of data in support of conservation of microcircuitry in the course of evolution and/or common developmental origins.

Author contributions: Y.W. and H.K. designed research; Y.W. and A.B.-P. performed research; Y.W. and H.K. analyzed data; and Y.W. and H.K. wrote the paper.

The authors declare no conflict of interest.

[1]To whom correspondence should be addressed. E-mail: wangyuan@uw.edu.

This article contains supporting information online at www.pnas.org/lookup/suppl/doi:10.1073/pnas.1006645107/-/DCSupplemental.

*A vertebrate brain has three primary portions: the prosencephalon (forebrain), mesencephalon (midbrain), and rhombencephalon (hindbrain), with the prosencephalon consisting of the telencephalon and diencephalon. The mammalian telencephalon contains cerebral cortex (traditionally and simplistically considered to consist of two major divisions, the neocortex and allocortex), claustrum, amygdala, and basal ganglia. The first three components are derived from the pallial sector of the developing telencephalon, whereas the basal ganglion is developed from the subpallial sector. In nonmammalian species, the pallial portion of the telencephalon is also divided into hyperpallium, mesopallium, and nidopallium based on location.

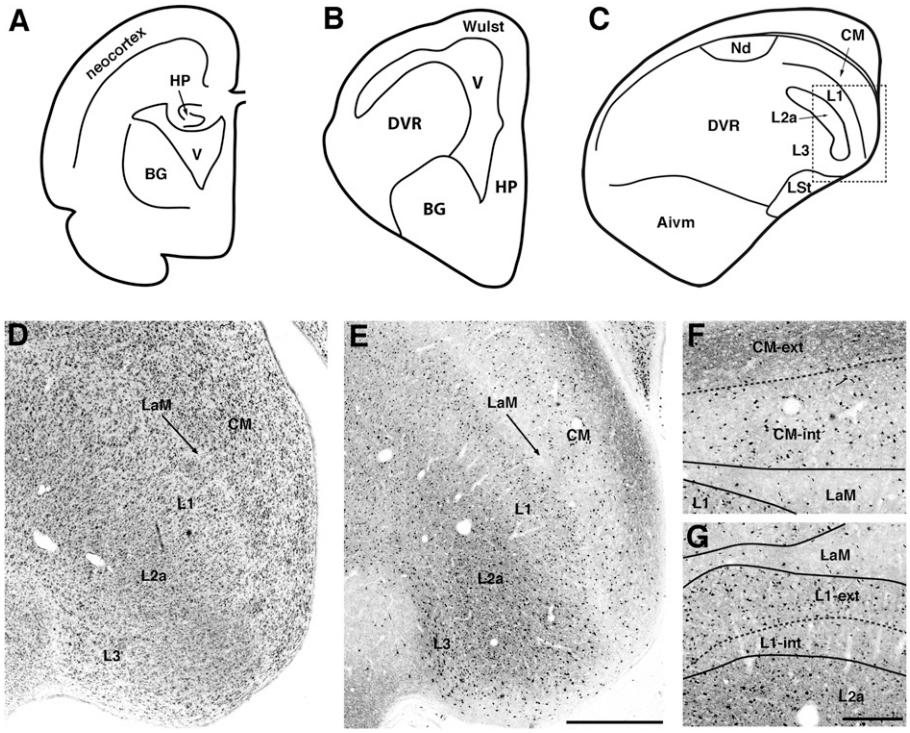

Fig. 1. The location and laminar organization of the Field L/CM complex in chicks. (*A*) A schematic drawing illustrates the organization of the mammalian telencephalon. (*B* and *C*) Schematic drawings illustrate the organization of the avian telencephalon and major components of the auditory telencephalon at the rostral (*B*) and caudal (*C*) levels. (*D* and *E*) Laminar arrangement of the Field L/CM complex is readily recognized in sections stained with either Nissl (*D*) or immunocytochemistry for parvalbumin (*E*). The location of the photomicrographs is comparable to the box in *C*. (*F*) CM externus and internus contain a high density of parvalbumin-immunoreactive axons and somata, respectively. (*G*) L1 externus contains a higher density of parvalbumin-immunoreactive neurons than L1 internus. Dorsal is up and medial is right in *A*–*E*. Photos in *F* and *G* were rotated ≈60 degrees counterclockwise. CM-ext, CM externus; CM-int, CM internus; L1-ext, L1 externus; L1-int, L1 internus. [Scale bars: 500 μm in *E* (applies to *D* and *E*); 200 μm in *G* (applies to *F* and *G*).]

In the present work, we provide evidence of a pattern of radial and columnar cellular circuitry within the auditory zone of the avian telencephalon, comparable to that found in the primary auditory cortex (A1) of mammals. The A1 in mammals is the first-order recipient of the ascending projections from the auditory thalamus, the ventral division of the medial geniculate nucleus (MGv) (32–35). The A1 is tonotopically organized, and neurons of one radial columnar module tend to respond to the same acoustic frequencies (20, 36, 37). In birds, the caudal mesopallium (CM) and three subnuclei of Field L (L1, L2a, and L3) are horizontally elongated cell groups with their long axes in the same orientation. Field L2a receives direct input from the thalamic nucleus ovoidalis (Ov), the avian homolog of the mammalian MGv, and then connects to CM, L1, and L3 (8, 38, 39). Functional magnetic resonance imaging has revealed that the avian Field L responds to a similar series of listening tasks as the human and other mammalian auditory cortices (15, 16). Using 2-deoxyglucose as an activity measure, Scheich and colleagues demonstrated a functional columnar organization that spans Fields L1, L2a, L3, and CM in response to sharply tuned auditory stimuli (40–42). However, whether this columnar pattern is a simple reflection of the tonotopic organization of thalamic inputs or a consequence of a similar internal organization of the avian Field L/CM complex as for the mammalian A1 remains unknown.

Using precise placements of a highly sensitive tracer into individual components of the chick Field L/CM complex, we examined the organization of the microcircuitry and cell morphology. We found that the avian Field L/CM complex displays a similar internal organization with comparable cell types and circuitries as those found in the mammalian A1. This similarity strongly argues for the homology of the two structures and might imply a conserved evolutionary origin of the mammalian neocortex from the non-mammalian pallium.

Results

Laminar Organization of the Field L/CM Complex. In birds, the auditory telencephalon consists of Field L in the caudal nidopallium, the CM, the dorsal nidopallium (Nd), and the ventromedial portion of the intermediate arcopallium (Aivm; Fig. 1*C*). Among these, the CM and three subdivisions of Field L (L1, L2a, and L3) are arranged in a series of laminae oriented approximately mediolaterally and separated by the mesopallial lamina (LaM; Fig. 1*D*). Both the CM and L1 are heterogeneous in cell density and alignment, and each can be further divided into external and internal sublayers. The CM externus is composed of loosely packed neurons oriented parallel to the surface of the ventricle. In contrast, the CM internus contains a high density of neurons without obvious alignment. The two sublayers of L1 resemble each other in general cytoarchitecture and are more difficult to differentiate in Nissl-stained sections. Neuron size in the CM and L1 are comparable, ranging from 70 to 170 μm^2 in area. The majority of the neurons in L2a are small (50–80 μm^2 in area). These cells are the smallest neurons in all of the layers and give L2a a granular appearance in Nissl-stained sections. These granule cells tend to align in vertical stacks perpendicular to the layers (Fig. S1). Neurons in L3 vary widely in size (50–250 μm^2 in area) and are distributed in a random pattern.

The Field L/CM complex displays a strong immunocytochemical staining for parvalbumin (Fig. 1*E*), similar to the mammalian A1 (43, 44). Individual layers of the chick CM and Field L, particularly the sublayers of the CM and L1, are readily apparent in sections stained with parvalbumin immunoreactivity. The CM

externus is characterized by heavily labeled terminals, whereas immunoreactivity in the CM internus is mostly somatic (Fig. 1*F*). Both sublayers of L1 contain labeled somata, with a notably higher density in the external division than in the internal division (Fig. 1*G*). Immunoreactivity in L2a and L3 was found in both somata and neuropils.

Columnar Organization of the Field L/CM Complex. To explore whether functional units in the Field L/CM complex are individual layers or vertical modules across all layers, using slice preparations of chick brains, we placed a highly sensitive tracer, biotinylated dextran amine (BDA), precisely into individual layers of the Field L and CM and mapped anterograde and retrograde transport of BDA within the complex. The resultantinjections were small (most commonly 80–200 μm in diameter). Regardless of the layers of deposition of the tracer, transport of BDA always formed a column that crossed all layers and was oriented perpendicular to the layers (Fig. 2 and Fig. S2). The column contained a central region across all layers with a relatively high density of labeled fibers and neurons and, in some cases, adjacent areas with scattered labeling of fibers and neurons. The width of the central region of the column varied from 300 to 500 μm. With few exceptions, retrogradely and anterogradely labeled neurons were located within or immediately adjacent to this central region. Individual or bundles of thick axons coursed within the column along its long axis, although sparse axons coursing obliquely away from the column were detected as well (arrows in Fig. 2*A*).

We also evaluated the lateral spread of the BDA transport by quantifying the size and shape of the region encompassing all labeled cell bodies (Table S1). The long axis of the region was oriented perpendicular to the layers and averaged 1,284 ± 322 μm (mean ± SD, $n = 21$; range, 492–1,868 μm). The average length of the short axis was 526 ± 194 μm (range, 193–894 μm). The short axes were 21–56% as long as the long axes (mean ± SD, 41 ± 10%).

Our data also demonstrate a remarkably similar main information stream within columnar modules in birds and mammals. In mammals, the information stream in A1 starts in layer IV, which receives tonotopic thalamic inputs from the MGv and then conveys information to more superficial layers, which in turn project to deeper layers (45). In birds, Field L2a is the principal recipient of thalamic input from Ov, the homolog of the mammalian MGv. After BDA injection into L2a, a prominent bundle of axons emerged from the injection site and coursed superficially through L1 and CM (Fig. 2*B*). Terminal-like processes were found in both the CM internus and L1, indicating a projection from L2a onto these superficial layers. This observation was confirmed by the presence of labeled neurons in L2a after BDA injections into L1 and/or the CM (Fig. 2*C*, Fig. S2 *A* and *B*, and Table S1).

After receiving inputs from L2a, the CM sends recurrent projections back to L1 and L2a, and many of these axons appear to continue into L3. Injections into the CM anterogradely labeled long descending axons that extended through all three layers of Field L (Fig. 2 *A*, *C*, and *D*). Some axons could be traced laterally beyond L3. Consistently, injections into these deeper layers (L1, L2a, and L3) retrogradely labeled neurons in the CM (Fig. 2*B*, Fig. S2 *B* and *D*, and Table S1). In contrast, L1 might not provide significant input to deeper layers. After BDA injections into L2a and/or L3, labeled neurons were consistently scarce in L1 (Fig. 2*B*, Fig. S2*D*, and Table S1); however, injections into either the CM or L1 demonstrated reciprocal connections between these two layers (Fig. 2*C* and Fig. S2*B*). A number of neurons in L3 may sent their axons or extend their dendrites to more superficial layers, as suggested by the presence of a low density of labeled neurons in L3 after BDA injections into the CM, L1, or L2a.

These radially oriented intrinsic connections within the Field L/CM complex were further confirmed at the individual cell level by visualizing the axonal morphology of the neurons filled intracellularly. Fig. 2 *E* and *F* shows two examples of this. The neuron illustrated in Fig. 2*E*, a nongranulous spiny neuron located in L2a, displayed a multipolar soma (255 μm^2 in area) and a 140 μm × 170 μm dendritic field. The main axon issued a number of axonal collaterals that mostly extended superficially toward the surface of the ventricle and arborized within L1 and the CM. One of these collateral extended deeply and formed a small arborization in L3. Three additional collaterals traveled within L2a without obvious arborization. We were not able to sample small

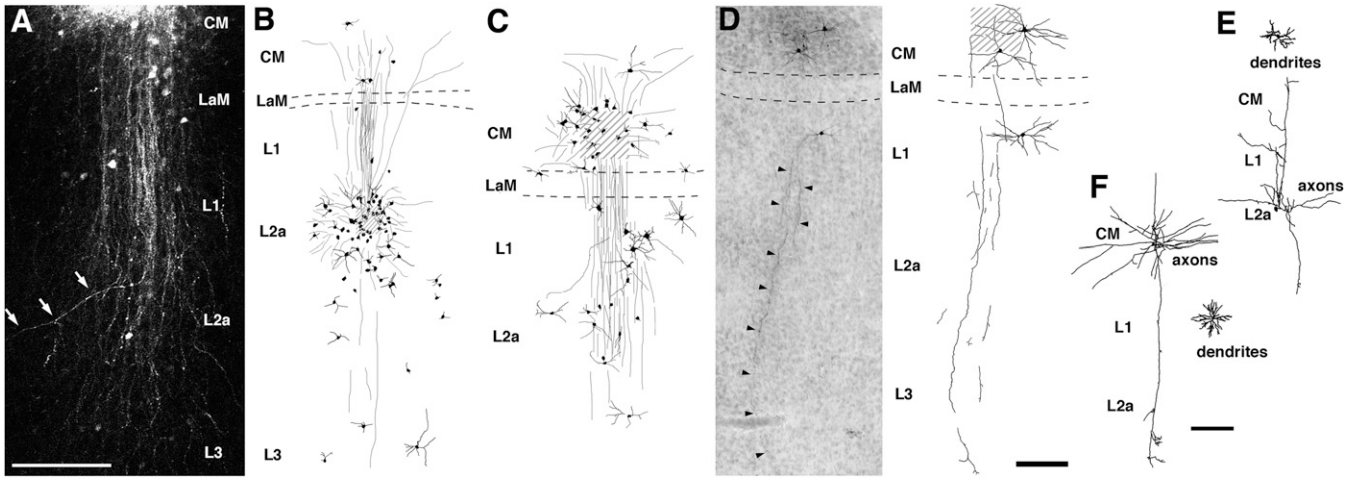

Fig. 2. Columnar organization of the Field L/CM complex in chicks. (*A*) Extended focus view of confocal microscopic Z-series of the labeling following an injection of BDA conjugated with rhodamine into CM. Note labeled axons and neurons were restricted within a column crossing all layers. White arrows point out an axonal collateral coursing obliquely away from the column. (*B–D*) Photomicrograph and camera lucida reconstruction of labeled neurons and fibers following an injection of BDA into Field L2a (*B*) and CM (*C* and *D*). Compared with the case in *C*, the injection site in *D* was much smaller and involved fewer neurons. Photomicrograph was taken from a Giemsa-counterstained section. Shaded areas indicate the center of an injection site. Dashed lines outline the location of LaM. Arrowheads in *D* point out the descending axons. See Fig. S2 for more reconstructions of injections. (*E* and *F*) Camera lucida reconstructions of intracellularly filled neurons in L2a (*E*) and CM (*F*). Dendrites and axonal arborization of each neuron are illustrated separately for clarity. Note the long radially oriented axonal collaterals in both cases. [Scale bars: 200 μm in *A*; 200 μm in *D* (applies to *B–D*); 200 μm in *F* (applies to *E* and *F*).]

granule cells in L2a with intracellular "sharp" electrodes because of the very small size of their somata. Fig. 2*F* shows a spiny stellate neuron (165 μm^2 in area) in the CM with a 180-μm × 200-μm dendritic field. The main axon issued collaterals coursing in all directions. Most collaterals were either short or did not exhibit obvious arborization before extending beyond the slices. The only exception was a long descending axon collateral that arborized prominently in L2a and L3.

Major Cell Types Responsible for Intrinsic Connections. The restricted distribution of labeled neurons in a column indicates that most, if not all, cell classes of the Field L/CM complex participate in the columnar organization. We reconstructed the somatodendritic morphology of several major cell types of labeled neurons after BDA injections. Notably, a major type of labeled neurons in L2a has a unique somatodendritic morphology (Fig. 3), identical in appearance to the small stellate granule cells in the mammalian layer IV described by Ramón y Cajal (46; fig. 385). The soma of these neurons in the chick L2a were tiny (mean, 76.3 ± 18.6 μm^2 in area; $n = 68$), with short and long axes of 7.7 ± 1.0 μm and 9.8 ± 1.5 μm, respectively. Between three and four extremely fine dendrites issued from the soma in all directions and formed a very restricted dendritic field, <100 μm in diameter. Some neurons displayed dendritic spines, and others appeared to have relatively smooth dendrites. Whereas most Golgi studies in mammals failed to identify this cell type, two studies (46, 47) successfully described the morphology of the granular cells in layer IV of the mammalian sensory cortex, which is very comparable to the granule cells identified in chicks. Sanides and Sanides (47) further noted that small stellate cells, which they called "short radiator" stellate cells, are the major cell types in layer IV in animals with a highly differentiated neocortex (also see ref. 49). These small stellate cells appear to be highly resistant to Golgi impregnation in humans (46), cats (48), and birds (11), and are difficult to sample with intracellular sharp electrodes.

A low density of large spiny and nonspiny multipolar and bipolar neurons was also labeled in L2a (Fig. 3*A*). These neurons' conspicuous thick dendrites and large dendritic fields distinguished them from the granule cells (Fig. S3). The somata ranged in average diameter from 10 to 18 μm. In contrast, these large neurons present the major cell types labeled in CM, L1, and L3 (Fig. S3). The dendritic patterns of these neurons varied among stellate, bipolar, and horizontal orientations. Occasionally, small stellate neurons were found in L3, morphologically similar to the granular cells in L2a. Pyramidal cells with long apical dendrites spanning several layers were not detected in the avian Field L/CM complex.

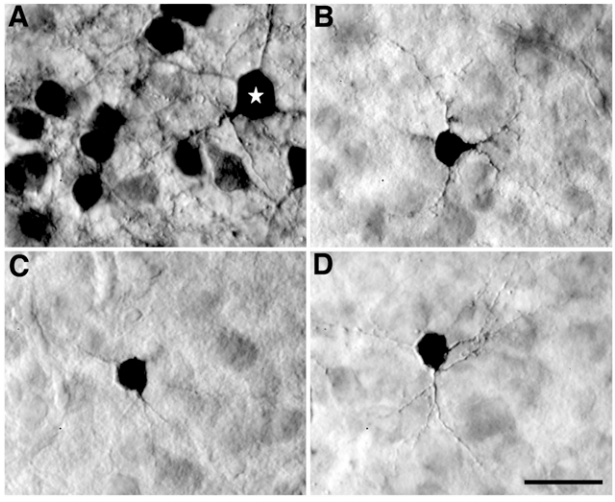

Fig. 3. Granule cells in Field L2a. (*A*) Labeled neurons in L2a following an injection of BDA into this layer. Small granule cells are the major cell type of labeled neurons in L2a. The white star indicates a large nongranule stellate cell. (*B–D*) Samples of granule cells in L2a labeled following injections into L1/L2 (*B*), CM (*C*), and L1 (*D*). Note the small cell bodies and fine and short dendrites. Nomarski-DIC photomicrographs were taken from Giemsa-counterstained sections. (Scale bar: 20 μm.)

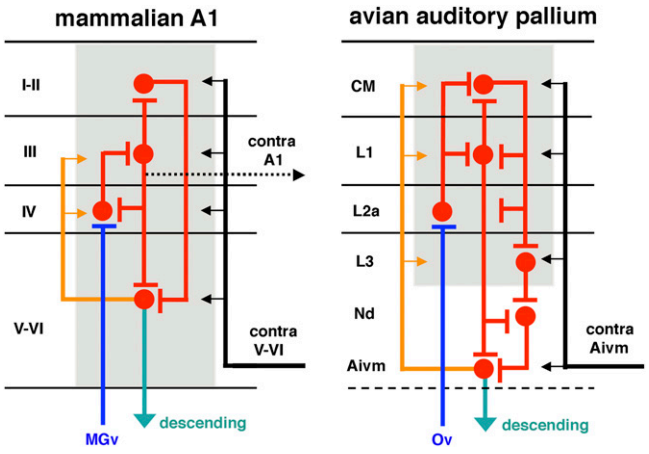

Fig. 4. Comparable laminar and columnar organization of the mammalian A1 (*Left*) and the avian auditory pallium (*Right*). Blue, red, and green lines and arrows indicate their thalamic inputs, intrinsic connections, and descending projections, respectively. Orange lines and arrows indicate recurrent projections from the deep layers to the more superficial layers. Black lines and arrows indicate reentrant projections from the other side of the brain. Innervation that is comparable to the projection from the mammalian layer III on the contralateral A1 (dotted black line) has not been identified in birds. Gray regions indicate columnar functional modules. Note that this schematic drawing illustrates only the major components of this intricate network.

Discussion

This study reveals remarkable similarities in the internal architecture of the microcircuitry of the avian auditory cortex and the primary auditory neocortex (A1) in mammals (Fig. 4). As in mammals, the avian Field L/CM complex, a prominent component of the auditory telencephalon, is composed of a number of layers in which auditory neurons interact via radially arrayed intrinsic connections.

Our results allow us to compare several layers of the mammalian A1 with specific cell groups in the avian auditory telencephalon. Specifically, the avian Field L2a corresponds to layer IV of the mammalian A1. Both structures contain densely packed small stellate neurons, also called granule cells. Their somata are separated by fibers into columns or clusters and electronically coupled in both squirrel monkey (50) and starling (11, 51). In both birds and mammals, dendrites of the granule cells are poorly developed in terms of thickness, length, and dendritic processes (46). Both the avian L2a and the mammalian layer IV are the direct targets of the primary ascending pathway from the auditory thalamus. Histochemically, the avian L2a contains a high density of parvalbumin immunoreactive neuropils, consistent with the staining pattern seen in layer IV of the mammalian A1. In addition, specific genes, such as eag/kch5, expressed within layer IV in mammals are similarly specifically expressed in the avian Field L2a.[†]

These conserved similarities suggest that the avian CM and L1 may represent a homolog of the superficial cortical layers in mammals, because they receive inputs from radially oriented axons

[†]Dugas-Ford J, Ragsdale CW, Nuclei in the avian dorsal ventricular ridge share molecular similarities with specific layers of the mammalian neocortex. Society for Neuroscience annual meeting, Oct. 23–27, 2004, San Diego, CA (abstr).

NEUROSCIENCE

of L2a neurons and in turn project back on L2a and other auditory regions in the telencephalon. Of note, this general pattern in chicks is consistent with previous studies in two other avian species (38, 39); see *SI Discussion* for more information. In particular, L1 (especially its external division) can be specifically compared with the mammalian layer III, because both provide major output from the superficial layers. In chicks, L1, but not the CM, contains neurons that project on the dorsal Nd (38). In addition, the L1 externus appears to be the major source of origin within the Field L/CM complex that innervates the ventromedial portion of the intermediate Aivm (Fig. S4). In mammalian A1, layer III sends axons to deeper layers within the column and, along with layers V and VI, provides exclusive laminar origin to the commissural connection between two A1s (45, 52).

Radially oriented intrinsic connections suggest that the functional unit of the avian Field L/CM complex is composed not of individual nuclei, but rather of columnar modules with interconnections across laminated layers. This suggestion was first advanced by Scheich and colleagues on the basis of their 2-deoxyglucose and physiological studies showing that units with the same or a similar best frequency are located in 2D neuronal planes perpendicularly across Field L and the CM (40–42). These results are directly comparable to observations in the mammalian A1, where all of the neurons within one columnar module tend to respond to the same or similar frequencies.

Not all layers of the mammalian A1 are equally represented in the Field L/CM complex. For example, a descending projection from the mammalian layers V and VI on the midbrain and thalamus is absent in the avian Field L and CM, but arises from the Aivm (38). The Aivm receives massive monosynaptic input from the L1 externus and polysynaptic input from L1 and L3 via the Nd (38), suggesting that the Nd and Aivm, along with L3, are critical components of the avian, equivalent to mammalian layers V and VI. Thus is supported by the finding that the Aivm shares some biochemical signatures with mammalian cortical layer V.[‡] In addition, the Aivm projects bilaterally on the Field L/CM complex (38). This bilateral projection can be compared with the recurrent intrinsic projection within the column from layers V and VI on the superficial layers and the reentrant projection from the contralateral layers V and VI on the superficial layers of the mammalian AI (45, 52).

This identical internal organization and intertelencephic connections of the avian Field L/CM complex and the mammalian A1 are consistent with these structures' equivalent functions in listening tasks (15, 16). This consistency strongly suggests the homology of the two structures and emphasizes the need to reevaluate our concepts of the uniqueness of cortical networks in mammals and their evolutionary origins. Other mammalian structures that have been suggested to be homologous to the avian Field L/CM complex do not exhibit similar internal organization, thalamic input, and function (*SI Discussion*). It is noteworthy that birds represent not a stage in the evolutionary history of mammals, but rather a parallel branch to mammals on the evolutionary tree. Notable differences in cytoarchitecture and organization between the avian auditory cortex and mammalian AI neocortex have been identified; for example, the avian Nd and Aivm do not exhibit laminar and columnar organization identified in the Field L/CM complex, even though they are comparable to mammalian layers V and VI in terms of connections and neurochemistry. In addition, we did not detect pyramidal cells with long apical dendrites spanning several layers in the avian Field L/CM. Mammalian pyramidal cells might have evolved from nonpyramidal neurons in stem reptiles (11), and long apical dendrites may be a mammal-specific representation.

In addition, our findings suggest that specific functional pathways in the brain can be analyzed in regard to their common phylogenetic origins. Although this is recognized to be the case for brain structures such as the spinal cord, brainstem, and olfactory bulb (46), it introduces a previously underutilized level of analysis to components involved in higher cognitive functions. The conserved evolution of the mammalian neocortex further supports the utility of birds as suitable animal model in studies of the organization, development, and information processing of the sensory systems, in addition to their current use in studies of motor systems, such as vocal control systems.

Materials and Methods

All experimental procedures were approved by the University of California San Diego's Animal Care and Use Committee and performed on White Leghorn chicks (*Gallus gallus*) of age <5 d. Extracellular BDA injections and intracellular filling were done in brain slice preparations (53). BDA (10%) was injected either by pressure (30–150 nL in volume) or iontophoretically (positive current of 2–10 μA for 10 min). Intracellular filling of biocytin (4%) into individual neurons was conducted iontophoretically (positive current of 2–3 nA for 3 min). Parvalbumin immunocytochemistry was performed against a primary antibody (1:10,000 dilution; Sigma-Aldrich; lot #017H4821). Localization of BDA, biocytin, and parvalbumin immunoreactivity was visualized by avidin-biotin-peroxidase or fluorescent methods. Sections were counterstained with Giemsa for identification of layers. Labeled neuronal structures with BDA or biocytin were traced with a camera lucida on a Zeiss WL microscope. Digital images of selected sections were captured with a Nikon microscope and D100 digital camera or an Olympus FV-300 confocal microscope. All of the measurements, including soma size and dimensions of tracer transports, were done on calibrated images, using Image software (National Institutes of Health). No corrections were made for tissue shrinkage. See *SI Materials and Methods* for more detailed information.

ACKNOWLEDGMENTS. We thank T. D. Albright, S. W. Bottjer, T. G. Gentner, W. Hodos, J. Isaacson, D. J. Perkel, E. W. Rubel, and S. M. Sherman for their critical comments on the manuscript. This work was supported by National Institute of Neurological Disorders and Stroke Grant NS 24560-15; National Institute of Mental Health Grant NH 60975-07; and National Institute on Deafness and Other Communication Disorders Grants DC 03829, DC 04661, DC 00018.

[‡]Dugas-Ford J, Ragsdale CW, Markers of mammalian layer 5 and 6 cells demonstrate the subnuclear architecture of the avian arcopallium. Society for Neuroscience annual meeting, Oct. 17–21, 2009, Chicago, IL (abstr).

1. Edinger L (1896) *The Anatomy of the Central Nervous System of Man and of Vertebrates in General* (F.A. Davis, Philadelphia).
2. Reiner A, et al.; Avian Brain Nomenclature Forum (2004) Revised nomenclature for avian telencephalon and some related brainstem nuclei. *J Comp Neurol* 473: 377–414.
3. Jarvis ED, et al.; Avian Brain Nomenclature Consortium (2005) Avian brains and a new understanding of vertebrate brain evolution. *Nat Rev Neurosci* 6:151–159.
4. Karten HJ, Shimizu T (1989) The origins of neocortex: Connections and lamination as distinct events in evolution. *J Cogn Neurosci* 1:291–301.
5. Karten HJ (1991) Homology and evolutionary origins of the "neocortex". *Brain Behav Evol* 38:264–272.
6. Karten HJ (1997) Evolutionary developmental biology meets the brain: The origins of mammalian cortex. *Proc Natl Acad Sci USA* 94:2800–2804.
7. Juorio AV, Vogt M (1967) Monoamines and their metabolites in the avian brain. *J Physiol* 189:489–518.
8. Karten HJ (1968) The ascending auditory pathway in the pigeon (*Columba livia*), II: Telencephalic projections of the nucleus ovoidalis thalami. *Brain Res* 11:134–153.
9. Karten HJ (1969) The organization of the avian telencephalon and some speculations on the phylogeny of the amniote telencephalon. *Comparative and Evolutionary Aspects of the Vertebrate Central Nervous System*, eds Petras JM, Noback CR (New York Academy of Science, New York), pp 164–179.
10. Nauta WJH, Karten HJ (1970) *The Neurosciences: Second Study Program*, ed Schmitt FO (Rockefeller Univ. Press, New York), pp 7–26.
11. Saini KD, Leppelsack HJ (1981) Cell types of the auditory caudomedial neostriatum of the starling (*Sturnus vulgaris*). *J Comp Neurol* 198:209–229.
12. Butler AB (1994) The evolution of the dorsal pallium in the telencephalon of amniotes: Cladistic analysis and a new hypothesis. *Brain Res Brain Res Rev* 19:66–101.
13. Medina L, Reiner A (2000) Do birds possess homologues of mammalian primary visual, somatosensory and motor cortices? *Trends Neurosci* 23:1–12.
14. Reiner A, Yamamoto K, Karten HJ (2005) Organization and evolution of the avian forebrain. *Anat Rec A Discov Mol Cell Evol Biol* 287:1080–1102.
15. Van Meir V, et al. (2005) Spatiotemporal properties of the BOLD response in the songbirds' auditory circuit during a variety of listening tasks. *Neuroimage* 25: 1242–1255.

16. Voss P, Gougoux F, Zatorre RJ, Lassonde M, Lepore F (2008) Differential occipital responses in early- and late-blind individuals during a sound-source discrimination task. *Neuroimage* 40:746–758.
17. Mountcastle VB (1957) Modality and topographic properties of single neurons of cat's somatic sensory cortex. *J Neurophysiol* 20:408–434.
18. Hubel DH, Wiesel TN (1969) Anatomical demonstration of columns in the monkey striate cortex. *Nature* 221:747–750.
19. Hubel DH, Wiesel TN (1977) Ferrier Lecture: Functional architecture of macaque monkey visual cortex. *Proc R Soc Lond B Biol Sci* 198:1–59.
20. Abeles M, Goldstein MH, Jr (1970) Functional architecture in cat primary auditory cortex: Columnar organization and organization according to depth. *J Neurophysiol* 33:172–187.
21. Aitkin L (1990) *The Auditory Cortex: Structural and Functional Bases of Auditory Perception* (Chapman & Hall, London).
22. Mountcastle VB (1997) The columnar organization of the neocortex. *Brain* 120: 701–722.
23. Jones EG (2000) Microcolumns in the cerebral cortex. *Proc Natl Acad Sci USA* 97: 5019–5021.
24. Diamond ME, Petersen RS, Harris JA, Panzeri S (2003) Investigations into the organization of information in sensory cortex. *J Physiol Paris* 97:529–536.
25. Horton JC, Adams DL (2005) The cortical column: A structure without a function. *Philos Trans R Soc Lond B Biol Sci* 360:837–862.
26. Rakic P (2008) Confusing cortical columns. *Proc Natl Acad Sci USA* 105:12099–12100.
27. Bruce LL, Neary TJ (1995) The limbic system of tetrapods: A comparative analysis of cortical and amygdalar populations. *Brain Behav Evol* 46:224–234.
28. Striedter GF (1997) The telencephalon of tetrapods in evolution. *Brain Behav Evol* 49: 179–213.
29. Puelles L (2001) Thoughts on the development, structure and evolution of the mammalian and avian telencephalic pallium. *Philos Trans R Soc Lond B Biol Sci* 356: 1583–1598.
30. Aboitiz F, Morales D, Montiel J (2003) The evolutionary origin of the mammalian isocortex: Towards an integrated developmental and functional approach. *Behav Brain Sci* 26:535–552, discussion 552–585.
31. Wullimann MF, Mueller T (2004) Teleostean and mammalian forebrains contrasted: Evidence from genes to behavior. *J Comp Neurol* 475:143–162.
32. Oliver DL, Hall WC (1978) The medial geniculate body of the tree shrew, *Tupaia glis*, II: Connections with the neocortex. *J Comp Neurol* 182:459–493.
33. Hashikawa T, Molinari M, Rausell E, Jones EG (1995) Patchy and laminar terminations of medial geniculate axons in monkey auditory cortex. *J Comp Neurol* 362:195–208.
34. Molinari M, et al. (1995) Auditory thalamocortical pathways defined in monkeys by calcium-binding protein immunoreactivity. *J Comp Neurol* 362:171–194.
35. Huang CL, Winer JA (2000) Auditory thalamocortical projections in the cat: Laminar and areal patterns of input. *J Comp Neurol* 427:302–331.
36. Merzenich MM, Knight PL, Roth GL (1975) Representation of cochlea within primary auditory cortex in the cat. *J Neurophysiol* 38:231–249.
37. Sally SL, Kelly JB (1988) Organization of auditory cortex in the albino rat: Sound frequency. *J Neurophysiol* 59:1627–1638.
38. Wild JM, Karten HJ, Frost BJ (1993) Connections of the auditory forebrain in the pigeon (*Columba livia*). *J Comp Neurol* 337:32–62.
39. Vates GE, Broome BM, Mello CV, Nottebohm F (1996) Auditory pathways of caudal telencephalon and their relation to the song system of adult male zebra finches. *J Comp Neurol* 366:613–642.
40. Bonke D, Scheich H, Langner G (1979) Responsiveness of units in the auditory neostriatum of the guinea fowl (*numida meleagris*) to species-species calls and synthetic stimuli, I: Tonotopy and functional zones of field L. *J Comp Physiol A* 132:243–255.
41. Scheich H (1983) Two columnar systems in the auditory neostriatum of the chick: Evidence from 2-deoxyglucose. *Exp Brain Res* 51:199–205.
42. Scheich H, Bonke BA (1981) Tone- versus FM-induced patterns of excitation and suppression in the 14-C-2-deoxyglucose–labeled auditory "cortex" of the guinea fowl. *Exp Brain Res* 44:445–449.
43. Brückner G, et al. (1994) Cortical areas are revealed by distribution patterns of proteoglycan components and parvalbumin in the Mongolian gerbil and rat. *Brain Res* 658:67–86.
44. Cruikshank SJ, Killackey HP, Metherate R (2001) Parvalbumin and calbindin are differentially distributed within primary and secondary subregions of the mouse auditory forebrain. *Neuroscience* 105:553–569.
45. Mitani A, et al. (1985) Morphology and laminar organization of electrophysiologically identified neurons in the primary auditory cortex in the cat. *J Comp Neurol* 235: 430–447.
46. Ramón y Cajal S (1911) *Histology of the Nervous System of Man and Vertebrates*; eds trans Swanson N, Swanson LW (1995)(Oxford Univ. Press, New York).
47. Sanides D, Sanides F (1974) A comparative golgi sutdy of the neocortex in insectivores and rodents. *Z Mikrosk Anat Forsch* 88:957–977.
48. Winer JA (1984) Anatomy of layer IV in cat primary auditory cortex (AI). *J Comp Neurol* 224:535–567.
49. Radtke-Schuller S (2001) Neuroarchitecture of the auditory cortex in the rufous horseshoe bat (*Rhinolophus rouxi*). *Anat Embryol (Berl)* 204:81–100.
50. Smith DE, Moskowitz N (1979) Ultrastructure of layer IV of the primary auditory cortex of the squirrel monkey. *Neuroscience* 4:349–359.
51. Saini KD, Leppelsack HJ (1977) Neuronal arrangement in the auditory field L of the neostriatum of the starling. *Cell Tissue Res* 176:309–316.
52. Code RA, Winer JA (1985) Commissural neurons in layer III of cat primary auditory cortex (AI): Pyramidal and non-pyramidal cell input. *J Comp Neurol* 242:485–510.
53. Wang Y, Luksch H, Brecha NC, Karten HJ (2006) Columnar projections from the cholinergic nucleus isthmi to the optic tectum in chicks (*Gallus gallus*): A possible substrate for synchronizing tectal channels. *J Comp Neurol* 494:7–35.

Supporting Information

Wang et al. 10.1073/pnas.1006645107

SI Discussion

In birds, both the medial and lateral portions of the CM are auditory telencephalic nuclei and connected with the Field L via monosynaptic and/or polysynaptic pathways. In chicks, the boundaries between the medial and lateral CM are ambiguous. Although our injections were located mostly in the more medial portion of the CM, we chose to describe the studied mesopallium region using the more general nomenclature "caudal mesopallium" for accuracy.

The traditional definition of the Field L2 in birds contains two divisions, a medial portion (L2a) and a more laterally located portion (L2b). The present study focuses on the similarities between the avian L2a and the mammalian A1, both of which are primary cortical targets of the tonotopically organized lemniscal auditory system. In contrast, neurons in L2b receive auditory inputs from separate ascending pathways and exhibit broad frequency tuning. The equivalent component of the avian L2b in mammals remains unknown. The organization and connection of L2b were not examined in the present study.

It is noteworthy that the general pattern of intrinsic connections of the Field L/CM complex in chicks is consistent with that reported in previous studies in two other avian species. In zebra finches, each subunit of the complex (CM, L1, L2a, L3) connects with another subunit through reciprocal connections (1). We identified the majority of these connections in chicks, but found no evidence of a substantial projection of L1 to other regions of the Field L. In chicks, L1 provides a major output layer of the complex, consistent with studies in pigeons (2). The pattern of the intrinsic connectivity of the complex appears to be less complicated in pigeons than in zebra finches and chicks, with only two projections identified (2). These discrepancies across studies might be due to interspecies variation and/or technical limitations. Given the complexity of the interconnections across layers, exploration of the intrinsic detailed organization of the complex must be conducted at the individual cell level.

The remarkable similarities between the mammalian A1 neocortex and the avian auditory cortex, as described above, emphasize the need to reevaluate our concepts of the uniqueness of cortical networks in mammals and their evolutionary origins. These findings further challenge the views that the avian Field L/CM complex is homologous to a part of the mammalian amygdala, endopiriform area, or claustrum instead of A1 (3–7). This reasoning is based on selective data from gene expression and development, as well as a disputed direct thalamic input to the amygdala and claustrum, which has been interpreted as being homologous to the avian Ov-Field L pathway. However, the thalamic inputs to the claustrum and amygdala originate from the medial and dorsal divisions of the medial geniculate nucleus, the posterior intralaminar nucleus, and the suprageniculate nucleus (8), which are components of the secondary or nonlemniscal auditory pathway characterized by polysensory inputs in addition to broad frequency tuning and lack of tonotopy (9). In contrast, the avian Field L/CM and the mammalian A1 are the major telencephalic targets of the lemniscal auditory pathway via the mammalian MGv and the avian Ov, which are characterized by sharp frequency tuning and tonotopic organization (9). The distinctly different sensory inputs of the mammalian amygdala/claustrum and the avian Field L/CM provide strong evidence against the proposed homology of these two structures. Another important difference between these two structures is that amygdala and claustrum do not display a columnar internal organization, although they do contain complex intrinsic connections among its subdivisions (10, 11).

SI Materials and Methods

All experimental procedures used in this study were approved by the University of California San Diego's Animal Care and Use Committee and were in accordance with International Committee of Medical Journal Editors policy. Experiments were performed on White Leghorn chicks (*Gallus gallus*) of age <5 d.

In Vitro BDA Tracing and Intracellular Filling in Slice Preparations. The procedure has been described previously (12). Forty-one chicks were anesthetized with a mixture of 40 mg/kg of ketamine and 12 mg/kg of xylazine, and then decapitated. Brain slices (300 μm thick) through the Field L/CM complex were prepared in a modified coronal plane that may best conform to the radial plane or orientation first suggested by Bonke et al. (13). Layers of the complex were readily identified in wet tissue as four approximately parallel bands of differing brightness. BDA was injected extracellularly into individual layers using a glass electrode filled with 10% BDA either by pressure (30–150 nL in volume) or iontophoretically (positive current of 2–10 μA for 10 min). Intracellular filling of individual neurons was conducted in different slices with an electrode (100–300 MΩ) filled with 4% biocytin in 0.3 M KAc. Cell penetration was indicated by a sudden negative voltage drop and cell discharges. Biocytin was iontophoresed into the neuron with 2–3 nA of positive current for 3 min. Only one cell was filled in a single slice. Localization of BDA and biocytin were subsequently visualized by the standard avidin-biotin-peroxidase method, and sections were counterstained with Giemsa for identification of layers. In total, 21 slices with identifiable lamination, a clean BDA injection site, and good transportation of the tracer were chosen from 65 injected slices for data analyses; the injection sites are listed in Table S1. Nine neurons were filled intracellularly with their somata located in CM ($n = 3$), L1 ($n = 1$), L2 ($n = 4$), and L3 ($n = 1$).

Parvalbumin Immunocytochemistry. The procedure has been described previously (12). In brief, two chicks were transcardially perfused with 0.9% saline followed by 4% paraformaldehyde. After postfixation and sucrose equilibration of the brain, 30-μm coronal sections were acquired using a freezing sliding microtome. Free-floating sections were incubated with primary antibody solution (1:10,000; Sigma-Aldrich; lot #017H4821) overnight at 4 °C, followed by biotinylated anti-IgG antibody (1:200) for 1 h at room temperature. Localization of parvalbumin immunoreactivity was subsequently visualized by the standard avidin-biotin-peroxidase method. The localization pattern in the Field L/CM complex was consistent in the two chicks.

Cell Reconstruction and Measurement. Tracing of labeled neuronal structures after BDA extracellular injections was done with a camera lucida on a Zeiss WL microscope from individual resectioned 80-μm-thick sections. Slices with injections of BDA-conjugated rhodamine were observed and reconstructed using an Olympus FV-300 confocal microscope. For intracellularly filled neurons, axons from three adjacent 80-μm-thick sections containing the soma were reconstructed to provide a more complete tracing of axonal collaterals. The cell reconstructions were performed before Giemsa counterstaining to avoid obscuring fine cellular processes. All of the measurements, including soma size and dimensions of tracer transports, were done on calibrated images captured with a black and white (B/W) CCD camera, using Image software (National Institutes of Health). No corrections were made for tissue shrinkage.

1. Vates GE, Broome BM, Mello CV, Nottebohm F (1996) Auditory pathways of caudal telencephalon and their relation to the song system of adult male zebra finches. *J Comp Neurol* 366:613–642.
2. Wild JM, Karten HJ, Frost BJ (1993) Connections of the auditory forebrain in the pigeon (*Columba livia*). *J Comp Neurol* 337:32–62.
3. Bruce LL, Neary TJ (1995) The limbic system of tetrapods: A comparative analysis of cortical and amygdalar populations. *Brain Behav Evol* 46:224–234.
4. Striedter GF (1997) The telencephalon of tetrapods in evolution. *Brain Behav Evol* 49: 179–213.
5. Puelles L (2001) Thoughts on the development, structure and evolution of the mammalian and avian telencephalic pallium. *Philos Trans R Soc Lond B Biol Sci* 356:1583–1598.
6. Aboitiz F, Morales D, Montiel J (2003) The evolutionary origin of the mammalian isocortex: Towards an integrated developmental and functional approach. *Behav Brain Sci* 26:535–552.
7. Wullimann MF, Mueller T (2004) Teleostean and mammalian forebrains contrasted: Evidence from genes to behavior. *J Comp Neurol* 475:143–162.
8. Doron NN, Ledoux JE (1999) Organization of projections to the lateral amygdala from auditory and visual areas of the thalamus in the rat. *J Comp Neurol* 412:383–409.
9. Hu B (2003) Functional organization of lemniscal and nonlemniscal auditory thalamus. *Exp Brain Res* 153:543–549.
10. Pitkänen A, Amaral DG (1998) Organization of the intrinsic connections of the monkey amygdaloid complex: Projections originating in the lateral nucleus. *J Comp Neurol* 398:431–458.
11. Cassell MD, Freedman LJ, Shi C (1999) The intrinsic organization of the central extended amygdala. *Ann N Y Acad Sci* 877:217–241.
12. Wang Y, Luksch H, Brecha NC, Karten HJ (2006) Columnar projections from the cholinergic nucleus isthmi to the optic tectum in chicks (*Gallus gallus*): A possible substrate for synchronizing tectal channels. *J Comp Neurol* 494:7–35.
13. Bonke D, Scheich H, Langner G (1979) Responsiveness of units in the auditory neostriatum of the guinea fowl (*numida meleagris*) to species-species calls and synthetic stimuli, I: Tonotopy and functional zones of field L. *J Comp Physiol A* 132: 243–255.

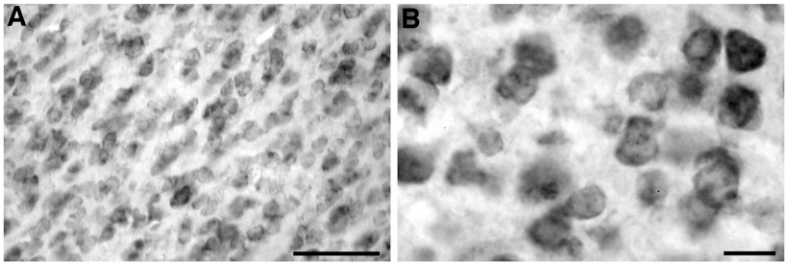

Fig. S1. Cytoarchitecture of Field L2a at low (*A*) and high (*B*) magnifications. Photos were taken from Nissl-stained sections and oriented the same way as in Fig. 1*D*, with dorsal at the top and medial to the right. The LaM was located dorsomedially to Field L2a. Note that granule cells in L2a tend to align in vertical stacks perpendicular to the layers. (Scale bar: 50 μm in *A*, 10 μm in *B*.)

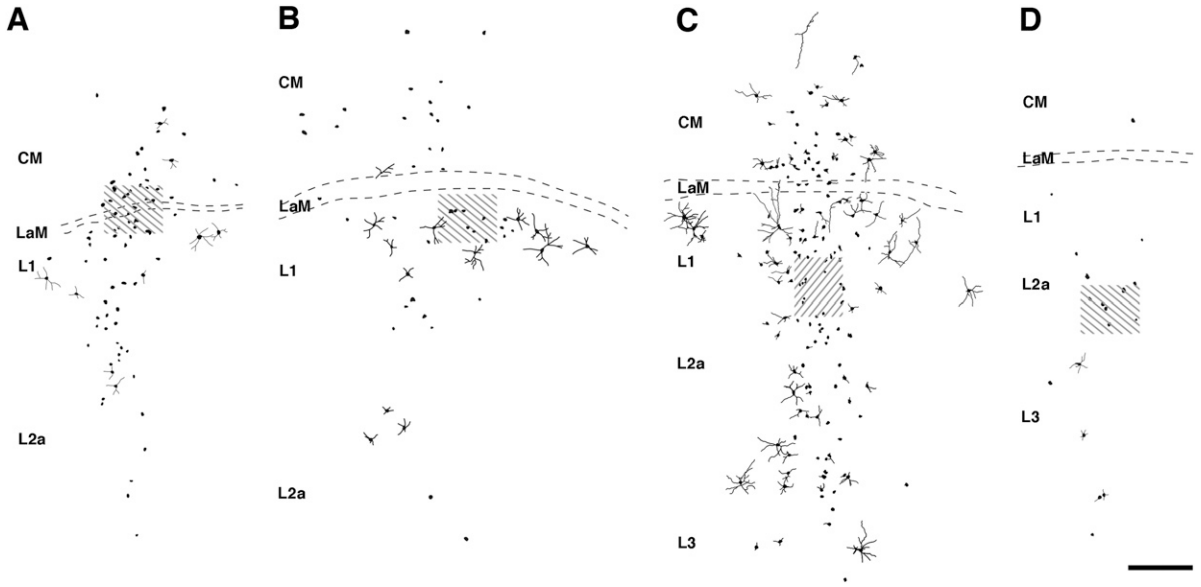

Fig. S2. Camera lucida reconstruction of labeled neurons after injection of BDA into CM/L1 (*A*), L1 (*B*), L1/L2a (*C*), and L2a/L3 (*D*). For clarity, labeled fibers are not shown. Note that the labeled neurons are located within a column crossing layers, regardless of the location and number of layers of deposition of the tracer. Shaded areas indicate the center of an injection site. Dashed lines outline the location of the LaM. (Scale bar: 200 μm.)

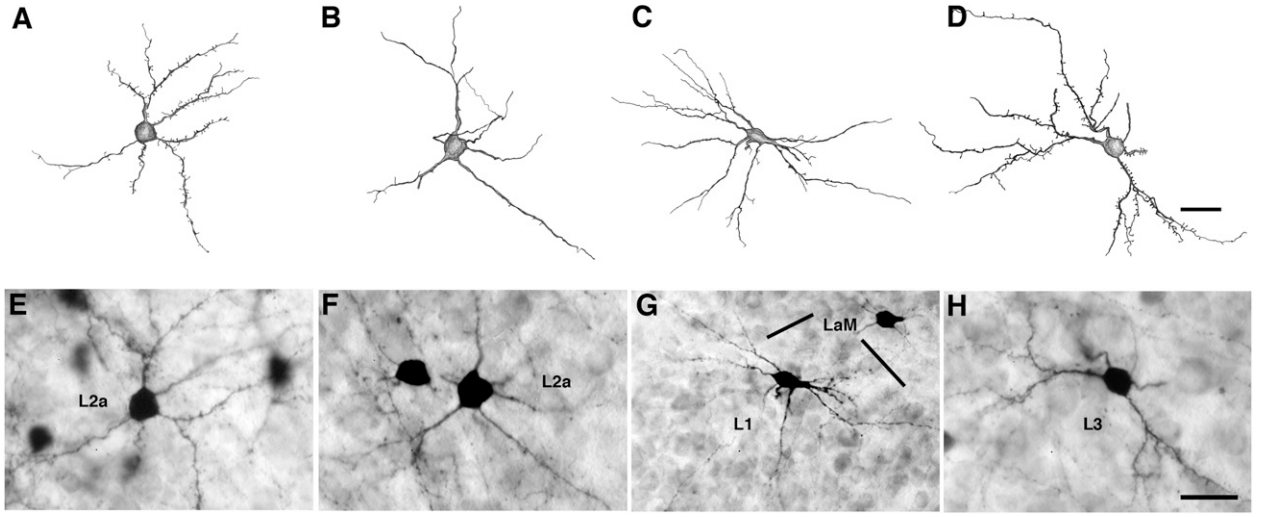

Fig. S3. Nongranule cell types in the Field L/CM complex revealed by BDA tracing studies. *A–D* show camera lucida reconstructions of the neurons illustrated in *E–H*, respectively. The neurons in *A* and *D* are spiny neurons, whereas those in *B* and *C* are relatively nonspiny. [Scale bars: 20 μm in *D* (applies to *A–D*), 20 μm in *H* (applies to *E–H*).]

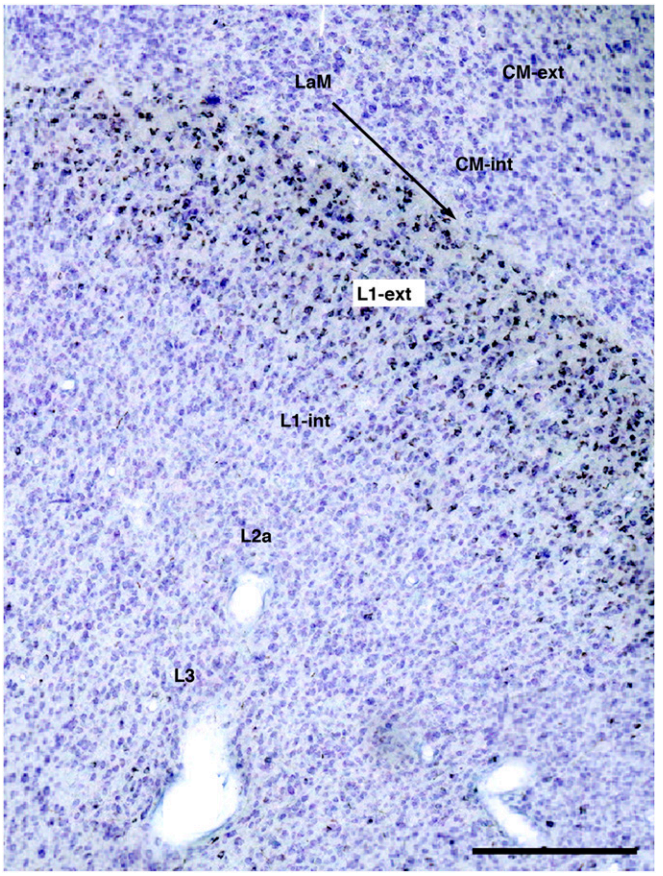

Fig. S4. Origin of the projection from the Field L/CM complex on Aivm. After an in vivo injection of CTB into the arcopallium, retrogradely labeled neurons within the Field L/CM complex were retricted to L1. Methods have been described in detail previously (4). The majority of the labeled neurons were found in L1 externus, with a very low density of labeled neurons detected in the internal portion of L1. There were no labeled neurons in CM, L2a, or L3, suggesting that L1 externus is a major output pathway of the Field/CM complex. The photo was taken from a Giemsa-counterstained section. Only CTB-containing cells were stained in black, with the remaining cells stained in blue. (Scale bar: 300 μm.)

Table S1. Injection site, injection method applied, and the distribution and number of labeled neurons following extracellular injections of BDA into the Field L/CM complex

Injection site	Injection method	Size of column (μm)*			Number of labeled neurons†			
		Long axis	Short axis	Ratio (%)	CM	L1	L2a	L3
CM	Pressure	1,251	573	46	—	11	12	4
CM	Pressure	1,135	635	56	—	11	28	0
CM	Pressure	1,291	587	45	—	17	9	1
CM	Iontophoresis	492	193	39	—	3	0	1
CM and L1-ext	Pressure	1,253	421	34	—	—	35	5
L1	Pressure	916	319	35	13	—	22	2
L1	Pressure	1,495	705	47	24	—	9	4
L1	Pressure	983	407	41	19	—	22	0
L1	Iontophoresis	1,405	465	33	22	—	6	4
L1-int and L2a	Pressure	1,705	894	52	49	—	—	10
L1-int and L2a	Iontophoresis	1,187	568	48	4	—	—	3
L1-int and L2a	Iontophoresis	1,748	765	44	14	—	—	5
L1 and L2a	Pressure	1,373	660	48	9	—	—	1
L1 and L2a	Iontophoresis	1,868	801	43	22	—	—	2
L2a	Pressure	1,653	341	21	16	1	—	10
L2a	Pressure	1,355	667	49	12	6	—	10
L2a	Pressure	1,359	631	46	4	1	—	5
L2a	Pressure	1,288	323	25	8	0	—	8
L2a	Pressure	1,190	551	46	15	0	—	6
L2a and L3	Pressure	1,212	281	23	10	1	—	—
L2a and L3	Iontophoresis	807	268	33	6	0	—	—

The cases are ordered by their injection sites. No notable differences in the patterns of labeling were detected between injections restricted to one layer and those involved with two layers.

*The extent of the column was determined by the distribution of labeled neurons. Labeled fibers mostly coursed within the column but also extended beyond its borders. The long and short axes of the column were measured from a single section for each case. Ratio refers to the length of the short axis divided by that of the long axis.

†The numbers of labeled neurons were counted for each layer of each case. Neurons were counted from either one section or two adjacent sections for each case. Labeled neurons in the layer(s) in which the injection site was located were not counted.